Higgs portal, fermionic dark matter, and a Standard Model like Higgs at 125 GeV

Laura Lopez-Honorez[1,*], **Thomas Schwetz**[1,†], **Jure Zupan**[2,‡]

[1] *Max-Planck-Institut für Kernphysik, Saupfercheckweg 1, 69117 Heidelberg, Germany*
[2] *Department of Physics, University of Cincinnati, Cincinnati, Ohio 45221,USA*

Abstract

We show that fermionic dark matter (DM) which communicates with the Standard Model (SM) via the Higgs portal is a viable scenario, even if a SM-like Higgs is found at around 125 GeV. Using effective field theory we show that for DM with a mass in the range from about 60 GeV to 2 TeV the Higgs portal needs to be parity violating in order to be in agreement with direct detection searches. For parity conserving interactions we identify two distinct options that remain viable: a resonant Higgs portal, and an indirect Higgs portal. We illustrate both possibilities using a simple renormalizable toy model.

1 Introduction

How dark matter (DM) couples to Standard Model (SM) particles is an open question. An interesting possibility is that the coupling of dark and visible sectors is through a Higgs portal [1–18]. The operator $(H^\dagger H)$ is one of the two lowest dimensional gauge invariant operators that one can write in the SM (the other one being the hyper-charge gauge field strength $B_{\mu\nu}$). Therefore, it is quite likely that also $(H^\dagger H)$–(dark sector) will be the lowest dimension operator connecting dark and visible sectors, and thus potentially the most important one.

Experimentally the Higgs portal is probed from two complementary directions. On the one hand, the new generation of direct DM detection experiments [19, 20] is starting to probe DM–nucleon scattering cross sections of roughly the size given by a single Higgs exchange with the SM Yukawa couplings to the quarks. On the other hand, the first hints of a SM-like Higgs boson signal were reported by the ATLAS and CMS collaborations. The hints of a signal are seen in several channels, pointing to a Higgs mass of roughly $m_h \sim 124 - 126$ GeV [21, 22], with the SM Higgs boson consistent with the current data at 82% C.L. [23], see also [24, 25]. Those hints are supported by recent results from D0 and CDF. For updates from ATLAS, CMS, D0, and CDF see [26].

*llopezho AT mpi-hd.mpg.de
†schwetz AT mpi-hd.mpg.de
‡jure.zupan AT cern.ch

In view of these experimental developments we revisit the Higgs portal to DM. In particular we focus on fermionic DM. The Higgs portals for the fermionic DM and the scalar DM are qualitatively different. For instance, if DM is a scalar, ϕ_{DM}, then the Higgs portal operator $(H^\dagger H)(\phi_{DM}^\dagger \phi_{DM})$ is renormalizable. The same is true if DM is a spin-1 particle. In contrast, if DM is a fermion, χ, then the Higgs portal necessarily proceeds through non-renormalizable interactions. The lowest dimensional Higgs portal in that case consists of two dim = 5 operators

$$Q_1 = (H^\dagger H)(\bar{\chi}\chi)\,, \qquad Q_5 = i(H^\dagger H)(\bar{\chi}\gamma_5\chi)\,, \tag{1}$$

which enter the effective Hamiltonian

$$H_{\text{eff}} = \frac{1}{\Lambda_1}Q_1 + \frac{1}{\Lambda_5}Q_5\,. \tag{2}$$

The mass scales $\Lambda_{1,5}$ are roughly the masses of the mediators for $\mathcal{O}(1)$ couplings between DM and the mediators. Since the DM–Higgs effective Hamiltonian is non-renormalizable, this means that a Higgs portal for fermionic dark matter necessarily requires a UV completion. In this paper we also consider situations when such UV completions are required in order to obtain a correct description of the DM phenomenology.

We first use the effective field theory (EFT) description of the Higgs portal (2) and derive consequences for each of the two operators $Q_{1,5}$. The parity conserving interaction, Q_1, is severely constrained by direct detection experiments. If only Q_1 is present in H_{eff} then one cannot obtain a small enough relic density consistent with the bound from XENON100 for DM masses below about 2 TeV [14]. In contrast, as we will show in section 2, the parity violating operator Q_5 is allowed by direct detection searches and the observed relic density can be obtained, see also [27]. Hence, when DM interactions are mediated by fields much heavier than $2m_\chi$ and $2m_h$ the EFT description is valid and we must conclude that the Higgs portal interactions for fermionic DM need to be parity violating ("pseudo-scalar Higgs portal"). Yet viable scenarios with parity conserving operators can be found when EFT breaks down. We identify two distinct options:

- "resonant Higgs portal" – where the dominant contribution is due to a resonant annihilation either through the Higgs or the mediator,
- "indirect Higgs portal" – where the DM annihilations into the mediator set the relic density and the Higgs portal only provides the link between the visible and dark sector thermal baths.

In section 3 we illustrate both of these two possibilities using a toy model – the minimal extension of the SM with a DM fermion χ and a real singlet ϕ see e.g. [4, 28].

2 Effective field theory considerations

Let us first assume that the mediators are heavy so that they can be integrated out. The Higgs portal is then given by eq. (2). We will be interested in the direct detection of

DM and in the annihilation of DM in the galactic halo. In both cases the DM particles entering the process are non-relativistic, with velocities typical of DM in the galactic halo, $\nu \sim 10^{-3}$. For annihilations in the early universe, responsible for obtaining the thermal relic density, DM is moderately relativistic.

The indirect and direct DM detection signals are given by the annihilation of two non-relativistic DM particles and the scattering of non-relativistic DM on the nuclei, respectively. For these two processes the two effective operators $Q_{1,5}$ behave in exactly the opposite way. For instance, the annihilation cross section is (for a Majorana fermion χ)

$$\sigma_{\rm ann} = \frac{1}{4\pi}\left[\frac{\left(1-4m_\chi^2/s\right)}{\Lambda_1^2}+\frac{1}{\Lambda_5^2}\right]\frac{f(m_\chi)}{\sqrt{1-4m_\chi^2/s}}, \tag{3}$$

which is in the non-relativistic limit

$$\sigma_{\rm ann} = \frac{1}{4\pi\nu}\left[\frac{\nu^2}{\Lambda_1^2}+\frac{1}{\Lambda_5^2}\right] f(m_\chi), \tag{4}$$

where ν is the velocity of each of the DM particles in the center-of-mass system (CMS). The contributions to annihilations from the parity conserving operator Q_1 are thus velocity suppressed, while parity violating contributions, due to Q_5, are unsuppressed. The function $f(m_\chi) \equiv \sum_i f_i$ sums the available final states i. For instance, for $m_\chi > m_h$ we have

$$f_h = \left(1+\frac{3m_h^2}{s-m_h^2}\right)^2\left(1-4m_h^2/s\right)^{1/2}, \qquad f_t = \frac{m_t^2}{s}\frac{(1-4m_t^2/s)^{3/2}}{(1-m_h^2/s)^2}, \tag{5}$$

for the decays to Higgs and top, respectively. For m_χ very heavy $f_h \to 1$ and $f_t \to 0$.

In the early universe, around the freeze-out temperature T_F we have $\nu^2 \sim T_F/m_\chi \simeq 1/20$, whereas in the galactic halo we have $\nu^2 \sim 10^{-6}$. As a consequence, for parity conserving interactions the annihilation cross section relevant for indirect detection signals is significantly suppressed compared to the one relevant for thermal freeze-out. In contrast, for parity violating interactions the annihilation cross section is independent of the velocity.

For direct detection the situation is exactly opposite. Integrating out the Higgs field, the scattering of DM on matter is given by an effective Hamiltonian

$$H = \sum_{i=1,5}\frac{C_i}{m_h^2}O_i, \tag{6}$$

where the two operators and Wilson coefficients are

$$O_{1,5} = \bar\chi\{1, i\gamma_5\}\chi\sum_q \frac{m_q}{v}\bar q q, \qquad C_{1,5} = \frac{v}{\Lambda_{1,5}}. \tag{7}$$

where $v = 246$ GeV is the Higgs vacuum expectation value (VEV). The cross section for χ scattering on the proton induced by the operator O_1 is then

$$\sigma(\chi p \to \chi p) = \frac{4}{\pi}\left(C_1 g_{Hp}\right)^2\left(\frac{m_{\rm red}}{m_h^2}\right)^2, \tag{8}$$

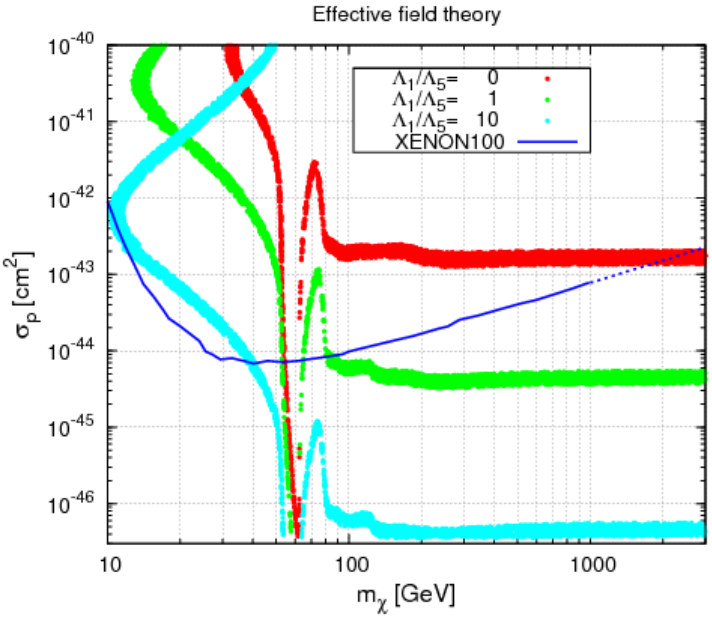

Figure 1: Proton–dark matter scattering cross section as a function of the dark matter mass in the effective field theory of eq. (2), as predicted by requiring that the correct relic density is obtained by thermal freeze-out. The scattering cross section is shown for several ratios of pseudo scalar coupling to scalar coupling Λ_1/Λ_5, and compared to the limit from XENON100 [19].

where $m_{\rm red} = m_p m_\chi/(m_p + m_\chi)$ is the reduced mass of the DM–proton system and

$$g_{Hp} = \frac{m_p}{v}\left[\sum_{q=u,d,s} f_q^{(p)} + \frac{2}{9}\left(1 - \sum_{q=u,d,s} f_q^{(p)}\right)\right] \approx 1.3 \times 10^{-3}\,, \tag{9}$$

see e.g., [29], where also values for $f_q^{(p)}$ are given. The operator O_5, on the other hand, induces a velocity suppressed scattering

$$\sigma(\chi p \to \chi p) = \frac{2}{\pi}\left(C_5 g_{Hp}\right)^2 \left(\frac{m_{\rm red}}{m_h^2}\right)^2 \nu^2. \tag{10}$$

where typically $\nu \sim 10^{-3}$. Hence in direct detection one obtains a velocity suppressed scattering cross section for parity violating interactions, but unsuppressed scattering for parity conserving ones.

This means that it is possible to find regions of $C_{1,5}$ parameter space with correct relic density but small enough direct detection signals. In fig. 1 we show the scattering cross section for different ratios of pseudo scalar coupling to scalar coupling Λ_1/Λ_5. For a fixed ratio and given DM mass we determine the sizes of Λ_i by requiring that the thermal relic density is obtained in the interval $0.09 < \Omega h^2 < 0.13$. For the thermal freeze-out calculations we use the `micrOMEGAs` [29, 30] public code, and we assume $m_h = 125$ GeV.

The curve for $\Lambda_1/\Lambda_5 = 0$ corresponds to parity conservation, i.e., pure scalar coupling. This case was considered for example in [2, 10, 14] and is incompatible with the bound from XENON100 [19] for DM masses $m_\chi \lesssim 2$ TeV. However, already for $\Lambda_1/\Lambda_5 \simeq 1$ the predicted cross section is below the XENON100 bound for $m_\chi \gtrsim 100$ GeV, while $\Lambda_1/\Lambda_5 \simeq 10$ leads to cross sections of about two to three orders of magnitudes below the limit.

Around $m_\chi \approx m_h/2 = 63$ GeV the effect of the s-channel resonance due to Higgs exchange is clearly visible in fig. 1. For DM masses below the resonance Higgs decays $h \to 2\chi$ become possible. The shape of the curves below the resonance is due to the Breit-Wigner form of the annihilation cross section. The contribution of $h \to 2\chi$ to the Higgs decay width allows for two solutions for Λ_i giving rise to the correct relic density at a given DM mass above a certain minimal mass and below the resonance. Note however, that in some cases Λ_i may become even smaller than m_χ and the EFT description may no longer be valid. Moreover, typically large branching fractions of the Higgs into DM are obtained in those cases. Therefore, the region below $m_h/2$ would be excluded by observing a Higgs with SM-like decay branching fractions.

Let us briefly mention constraints from indirect detection. In the case of pure scalar interactions DM annihilations are ν^2 suppressed. In the early universe at freeze-out $\nu^2 \simeq 1/20$, whereas in the galactic halo we have $\nu^2 \sim 10^{-6}$. This leads to a negligible signal for indirect detection experiments. As soon as the pseudo-scalar coupling becomes comparable to the scalar one, the annihilation cross section is dominated by pseudo-scalar interactions with $\sigma\nu$ independent of the velocity, see eq. (4). Therefore, in the latter case, the annihilation cross section will be the "thermal" one with $\sigma\nu \simeq 3 \times 10^{-26}\,\mathrm{cm^3 s^{-1}}$. Current data from FERMI-LAT and BESS-Polar II disfavour such cross sections for $m_\chi \lesssim 30$ GeV [31, 32]. Since here we are restricted to DM masses $m_\chi \gtrsim 60$ GeV current limits from indirect detection do not constrain this model.

Let us mention that monojet searches for dark matter at colliders [33, 34] will apriori not constrain further this EFT model of dark matter. Limits on spin-independent interactions from recent LHC data [35, 36] are much weaker than Xenon bounds in the region of interest.

3 Beyond the EFT framework

3.1 The toy model

Now we move to situations which cannot be described by the EFT. In order to illustrate when it is possible to have a viable fermionic DM Higgs portal we consider a simple UV completion by introducing a real scalar singlet that will act as mediator particle[1]. For simplicity we consider a Majorana fermion χ as DM, with $\chi = \chi_L + \chi_L^c$ in 4-component

[1] For alternative UV completions see e.g. [37, 38].

notation. (All our arguments will equally apply to the Dirac case.) We denote the SM Higgs doublet by H and the real singlet scalar by φ. The relevant terms in the Lagrangian are

$$\begin{aligned}\mathcal{L} = &\frac{1}{2}\bar{\chi}_L(i\gamma_\mu\partial^\mu - \mu_\chi - g\varphi)\chi_L^c + \text{h.c.} \\ &+ (D_\mu H)^\dagger D^\mu H + \frac{1}{2}\partial_\mu\varphi\partial^\mu\varphi - V(\varphi, H)\,,\end{aligned} \tag{11}$$

Here D^μ is the SM gauge-covariant derivative, $V(\varphi, H)$ is the Higgs potential, and we allow the coupling constant g and the mass parameter μ_χ to be complex. Let us work in unitary gauge and expand H and φ around their VEVs:

$$H = \frac{1}{\sqrt{2}}\begin{pmatrix} 0 \\ h + v_1 \end{pmatrix}, \qquad \varphi = \phi + v_2 \tag{12}$$

where $v_1 = 246$ GeV. By performing a phase transformation $\chi_L \to e^{i\alpha/2}\chi_L$ with $\alpha = \text{Arg}(\mu_\chi + gv_2)$ we find that the physical mass of χ corresponds to $m_\chi = |\mu_\chi + gv_2|$. The phase of g relative to the mass term determines the scalar (S) or pseudo-scalar (P) nature of the Yukawa coupling:

$$g_S = \text{Re}(ge^{-i\alpha})\,, \qquad g_P = \text{Im}(ge^{-i\alpha})\,. \tag{13}$$

A non-zero value of g_P violates parity. The mass term and the interaction terms for the Majorana fermion χ become thus:

$$\mathcal{L}_\chi = -\frac{1}{2}\left(m_\chi\bar{\chi}\chi + g_S\phi\bar{\chi}\chi + ig_P\phi\bar{\chi}\gamma_5\chi\right)\,. \tag{14}$$

As discussed in the previous section the pseudo-scalar coupling leads to suppressed rates in direct detection. Therefore, it is always possible to consider the situation of $g_S \ll g_P$ in order to reconcile the annihilation cross section required for the relic density with stringent bounds on the DM–nucleon scattering cross section. In the following we discuss alternative ways to achieve this goal, and therefore we assume in this section parity conservation, $g_P = 0$, keeping always in mind the possibility of parity violation on top of the mechanisms discussed here.

The Higgs potential is

$$V(\varphi, H) = -\mu_H^2 H^\dagger H + \lambda_H (H^\dagger H)^2 - \frac{\mu_\varphi^2}{2}\varphi^2 + \frac{\lambda_\varphi}{4}\varphi^4 + \frac{\lambda_4}{2}\varphi^2 H^\dagger H \tag{15}$$

$$+ \frac{\mu_1^3}{\sqrt{2}}\varphi + \frac{\mu_3}{2\sqrt{2}}\varphi^3 + \frac{\mu}{\sqrt{2}}\varphi(H^\dagger H)\,, \tag{16}$$

where the λ_4 and μ terms provide the Higgs portal between the dark and SM sectors. In order to keep the expressions simple we set in the following always $\mu_1 = \mu_3 = 0$. Those terms will not introduce new physical effects and therefore all features relevant for our discussion can be captured within this restricted framework.

In general mixing between h and ϕ will be induced, with physical mass states H_1 and H_2 and a mixing angle α with

$$\tan 2\alpha = \frac{\sqrt{2}\mu v_1 + 2\lambda_4 v_1 v_2}{2\lambda_H v_1^2 - 2\lambda_\phi v_2^2 + \mu v_1^2/(2\sqrt{2}v_2)} \,. \tag{17}$$

We adopt the convention that for $\alpha \to 0$, H_1 corresponds to h. Hence, for small mixing and $m_{H_1} = 125$ GeV, $H_1 \approx h$ becomes a SM-like Higgs. All direct processes coupling χ to the SM are proportional to $\sin^2 2\alpha$ and therefore the mixing angle plays a crucial role for DM signals.

3.2 Direct detection

DM scattering on nuclei relevant for direct detection is mediated via t-channel exchange of the Higgs mass eigenstates H_1 and H_2. Hence, scattering is spin-independent. The elastic scattering cross section σ_p of χ off a proton p is obtained as

$$\sigma_p = \frac{g_S^2 \sin^2 2\alpha}{4\pi} m_{\rm red}^2 \left(\frac{1}{m_{H_1}^2} - \frac{1}{m_{H_2}^2}\right)^2 g_{Hp}^2 \,. \tag{18}$$

The typical size of the scattering cross sections is

$$\sigma_p \approx 5 \times 10^{-43}\,{\rm cm}^2\, g_S^2 \sin^2 2\alpha \left(\frac{m_{\rm red}}{1\,{\rm GeV}}\right)^2 \left(\frac{1}{m_{H_1}^2} - \frac{1}{m_{H_2}^2}\right)^2 (100\,{\rm GeV})^4 \,. \tag{19}$$

This number has to be compared to the limit from XENON100, which is $\sigma_p \lesssim 10^{-44}\,{\rm cm}^2$ for $m_\chi \simeq 50$ GeV [19]. Hence, couplings of order one and large mixing are in tension with the bound. In eq. (18) we take into account only the scalar coupling g_S. Similar to the EFT case discussed above, for pseudo-scalar interactions the cross section is suppressed by $\nu^2 \sim 10^{-6}$.

3.3 LHC Higgs signatures

In order to define a SM-like Higgs h with $m_{H_1} = 125$ GeV, we will use the notion of signal strength reduction factor in the event number of a specific final state of the Standard Model, X, in the Higgs boson decay, see e.g. [15, 28, 39]. The latter is defined as:

$$r_i \equiv \frac{\sigma_{H_i} {\rm Br}_{H_i \to X}}{\sigma_{H_i}^{\rm SM} {\rm Br}_{H_i \to X}^{\rm SM}} \tag{20}$$

with $i = 1, 2$ and where σ_{H_i} and ${\rm Br}_{H_i \to X}$ are the Higgs production cross section and branching ratio of $H_i \to X$, respectively, while $\sigma_{H_i}^{\rm SM}$ and ${\rm Br}_{H_i \to X}^{\rm SM}$ are the same quantities for a Standard Model Higgs with $m_h = m_{H_i}$. One obtains

$$r_1 = \cos^4\alpha \, \frac{\Gamma_{H_1}^{\rm SM}}{\Gamma_{H_1}} \quad \text{and} \quad r_2 = \sin^4\alpha \, \frac{\Gamma_{H_2}^{\rm SM}}{\Gamma_{H_2}} \tag{21}$$

where α denotes the Higgs mixing angle, $\Gamma_{H_i}^{\rm SM}$ is the total decay width of a SM Higgs of mass $m_h = m_{H_i}$ and Γ_{H_i} is the total decay width of H_i including the decay into $H_{j\neq i}$ and χ. In order to have a SM-like Higgs we require small mixing α and identify H_1 with the SM Higgs h with $m_{H_1} = 125$ GeV. In practice, we will require that $r_1 > 0.9$ and $r_2 < 0.1$. The latter constraint is imposed to respect the fact that no indication of a second Higgs-like particle is seen at LHC. In the model under consideration typically requiring $r_1 > 0.9$ automatically leads to $r_2 < 0.1$. Note that eq. (21) is independent of the Higgs decay channel X. Therefore, we can compare r_i directly with the ATLAS/CMS results on the signal strength reduction factor obtained from a combination of all search channels.

3.4 Numerical results

We have performed a numerical scan over the parameters of this model using `micrOMEGAs` [29, 30]. We assume $m_{H_1} = 125$ GeV and set $g_P = 0$. Then we scan randomly over $m_\chi, g_S, v_2, \mu, \lambda_4$, and m_{H_2} or λ_ϕ as free parameters. In order to ensure perturbativity, we impose that the absolute value of the couplings $\lambda_4, \lambda_\phi, \lambda_H$ and g_S are smaller than π. For the scalar potential to be bounded from below, we imposed $\lambda_\phi, \lambda_H > 0$ and $\lambda_4 > -2\sqrt{\lambda_\phi \lambda_H}$. We also assume that χ is the only dark matter candidate that gives rise to a relic density $0.09 < \Omega h^2 < 0.13$ obtained by thermal freeze-out. If not mentioned otherwise, we scanned the following range of parameters: 5 GeV$\leq m_{H_2}, m_\chi \leq 10^4$ GeV, $10^{-4}\,\text{GeV} \leq |\mu|, v_2 \leq 10^4$ GeV, and $10^{-5} \leq |\lambda_4|, |g_S| \leq \pi$. We identify two viable parity conserving Higgs portals.

3.4.1 Resonant Higgs portal

We first assume $m_{H_1} \ll m_{H_2}$ and fix $m_{H_2} = 2000$ GeV. Requiring the correct relic abundance we show the predicted direct detection scattering cross section in fig. 2 compared to the bound from XENON100. For DM masses $m_\chi \lesssim 500$ GeV the mediator mass is still "heavy" and we recover roughly the EFT behaviour from fig. 1. However, we clearly observe the suppression of the direct detection rate when $m_\chi \approx m_{H_1}/2$ or $m_{H_2}/2$, where there is an s-channel resonance for annihilations, allowing for small coupling constants while maintaining the correct relic abundance. The red dots in fig. 2 correspond to a signal strength modifier for the Higgs signal at LHC of $r_1 < 0.9$. Hence, those points would be excluded by confirming a SM-like Higgs at 125 GeV, while for the green points we have $r_1 > 0.9$, showing that close to the resonances we can easily have parity conserving fermionic Higgs portal DM consistent with a SM-like Higgs.

3.4.2 Indirect Higgs portal

Let us now discuss the region $m_\chi > m_{H_2} = 2$ TeV in fig. 2. In this case annihilation of χ into the mediator becomes kinematically allowed. There are t- and u-channel diagrams contributing to this annihilation channel, which are independent of the mixing angle α

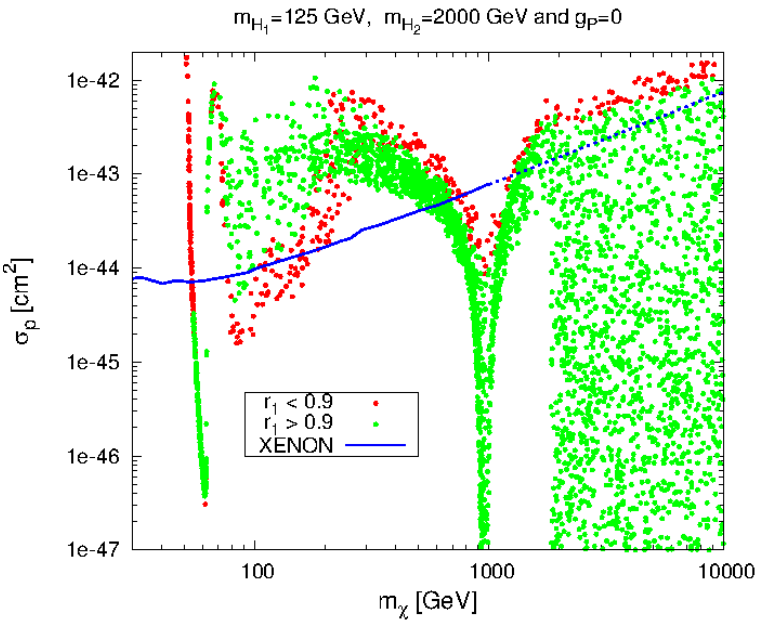

Figure 2: Proton–DM scattering cross section as a function of the dark matter mass in the Higgs portal model for $m_{H_1} = 125$ GeV, $m_{H_2} = 2$ TeV, and $g_P = 0$. The green points correspond to a SM-like H_1 with an LHC Higgs signal strength modifier $r_1 > 0.9$, while the red points have $r_1 < 0.9$. The points above the blue line are excluded at 95% CL by the XENON100 experiment [19]. This exclusion limit has been extended for $m_\chi > 1$ TeV assuming a linear dependence in m_χ.

and only depend on the coupling g_S. Assuming pure scalar coupling and $m_{H_{1,2}} \ll m_\chi$ we find

$$\sigma_{\chi\chi\to\phi\phi} = \frac{3 g_S^4 \nu}{32\pi m_\chi^2} \qquad (u\text{- and } t\text{-channel diagrams}), \tag{22}$$

where ν is the χ velocity in the CMS. The relic density is obtained when the reaction $\chi\chi \leftrightarrow \phi\phi$ freezes out. (Note that for small mixing we have $\phi \sim H_2$.) This fixes essentially the coupling g_S, while leaving the Higgs mixing α unconstrained. Since the direct detection cross section is proportional to $\sin^2(2\alpha)$, essentially any value for σ_p below the XENON100 bound can be obtained[2], as confirmed in fig. 2 for $m_\chi > 2$ TeV. We study this situation in more detail in the following.

For $m_{H_{1,2}} < m_\chi$ the exchange of light scalar fields $H_{1,2}$ between the two annihilating dark matter particles creates a long range attractive potential (long range compared to

[2]At 1-loop DM–nucleus scattering is induced also for zero Higgs mixing, if $\lambda_4 \neq 0$, giving a lower bound on the scattering cross section. The Wilson coefficient in eq. (8) is in this case $C_1 = (\sqrt{2} g_S^2 \lambda_4 / 16\pi^2)(m_\chi v_1 / m_\phi^2) f(x)$, with $x = m_\chi^2/m_\phi^2$ and $f(x) = 1/(1-x) - x\log(x)/(1-x)^2$ so that $f(0) = 1$. Note that this means that for zero $\phi - h$ mixing the suppression scale is $\Lambda_1 \sim 16\pi^2 m_\phi^2/m_\chi$ for $\mathcal{O}(1)$ couplings. For typical parameter choices the loop process induces tiny cross sections below $10^{-50}\,\mathrm{cm}^2$.

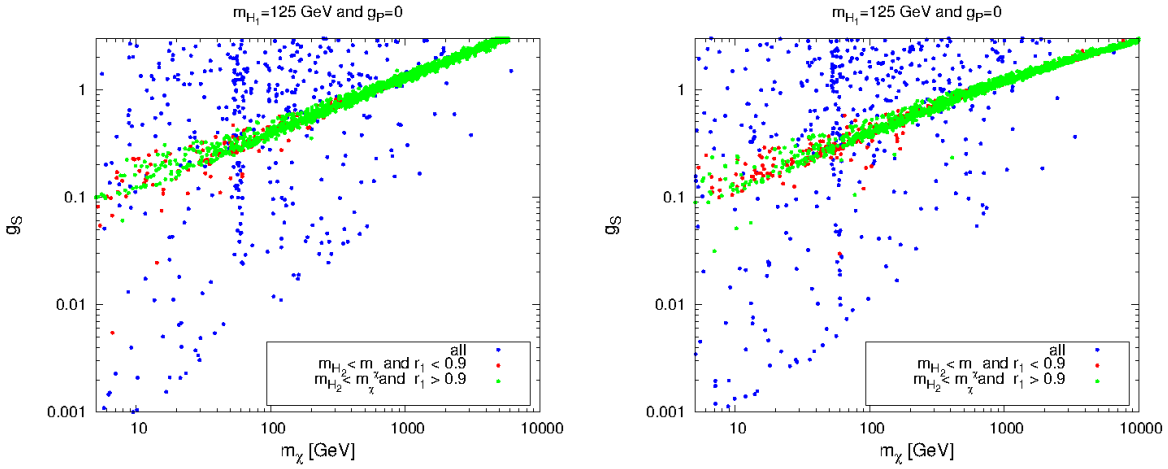

Figure 3: Parameter choices giving rise to a relic density in the WMAP range in the Higgs portal model with $m_{H_1} = 125$ GeV and $g_P = 0$. Green and red points correspond to $m_{H_2} < m_\chi$ with a more ($r_1 > 0.9$) or less ($r_1 < 0.9$) SM Higgs-like H_1, respectively. We show the scalar coupling g_S as a function of the dark matter mass without (left) and with (right) Sommerfeld enhancement for the relic density computation. For illustration, we also show the points with $m_{H_2} > m_\chi$ (blue points).

the Compton wavelength of χ). As a result there is a *Sommerfeld* enhancement of the dark matter annihilation cross-section [40]. This velocity dependent effect has been studied in detail in several references, see e.g. [41–43] (see also [44] for a very similar framework). In the calculations of the dark matter relic density we estimate the Sommerfeld enhancement averaged over a thermal distribution at freeze-out temperature T_f following [45]. We assume that the cross section determining the dark matter relic abundance is p-wave suppressed. The thermally averaged Sommerfeld factors $\bar{S}_\Phi(x_f)$ due to $\Phi = H_1$ and H_2 exchanges are functions of the couplings $\alpha_{H_1} = (g_S \sin\alpha)^2/(4\pi)$ and $\alpha_{H_2} = (g_S \cos\alpha)^2/(4\pi)$, respectively, and of the dimensionless parameters $\epsilon_\Phi = m_\chi/(\alpha_\Phi m_\Phi)$ and $x_f = m_\chi/T_f$ (all in the notation of [45]). Let us emphasize that in our toy model dark matter does couple to two mediators, in which case the computation of the exact Sommerfeld factor is more involved [46] than the results in [45]. In most of the cases considered here, only one of the two scalars leads to a non-negligible Sommerfeld correction $\bar{S}$ and the relic density is taken to be $\Omega_\chi h^2 \propto 1/(\bar{S}\langle\sigma v\rangle)$, where the thermal averaged annihilation cross-section $\langle\sigma v\rangle$ is obtained with `micrOMEGAs`. If both H_1 and H_2 lead to a non negligible thermally averaged Sommerfeld factor, then $\bar{S}$ is taken to be the largest of the two [3].

For masses $m_\chi \lesssim 100$ GeV, no Sommerfeld enhancement of the thermal averaged annihilation cross-section is observed. For $m_\chi \gtrsim 100$ GeV, $\bar{S}_{H_2}$ can become larger than one and take values up to 4.5. Above $m_\chi \sim 1$ TeV, we observe values of $\bar{S}_{H_1} \geq 1$ going

[3]Notice that in the particular framework of Ref. [46] it was shown that the exchange of multiple mediators can increase the Sommerfeld enhancement in the off-resonant region by $\sim 20\%$.

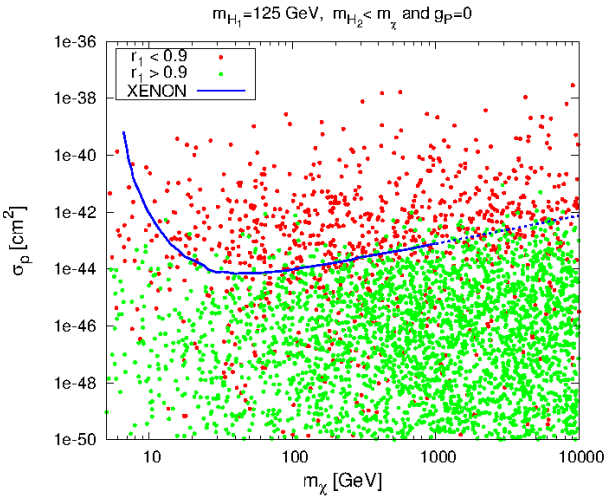

Figure 4: Parameter choices giving rise to a relic density in the WMAP range in the Higgs portal model with $m_{H_1} = 125$ GeV and $g_P = 0$. Green and red points correspond to $m_{H_2} < m_\chi$ with a more ($r_1 > 0.9$) or less ($r_1 < 0.9$) SM Higgs-like H_1, respectively. We show the DM–proton scattering cross section as a function of the dark matter mass for $m_{H_2} < m_\chi$ only. The points above the blue line are excluded at 95% CL by the XENON100 experiment [19]. This exclusion limit has been extended for $m_\chi > 1$ TeV assuming a linear dependence in m_χ.

up to 2. The main impact of the Sommerfeld enhancement is to allow for smaller values of the couplings g_S at a given mass m_χ in order to account for the correct relic density. This is illustrated in fig. 3 where we show the DM coupling to the scalar singlet, g_S, as a function of the DM mass with and without Sommerfeld enhancement. For the case $m_{H_2} < m_\chi$ (red and green points) we observe a clear correlation consistent with $g_S^2 \propto m_\chi$. This is expected when the relic density is driven by the process $\chi\chi \leftrightarrow \phi\phi$ according to eq. (22). Also notice the relative flattening of the $g_S^2 - m_\chi$ correlation for m_χ in the right panel of fig. 3. This is due to the presence of the Sommerfeld enhancement factor allowing for smaller coupling at a given value m_χ in order to still be consistent with WMAP data.

In fig. 4, we show the direct detection cross section requiring $m_{H_2} < m_\chi$. We see that the χ-nucleon scattering cross section can have vastly varying values. It can be well below the XENON100 bound, while still accounting for the correct relic density. This confirms that the size of the DM annihilation cross section (which controls the relic density) is no longer related to the strength of DM interactions with the SM. In fig. 4 the green points have $r_1 > 0.9$, which means that H_1 will look like a SM Higgs at the LHC, while the red points have a suppressed Higgs signal, $r_1 < 0.9$. We observe that the $r_1 > 0.9$ requirement tends to keep the scattering cross section below the XENON100 limit.

In the relic density calculation we have assumed that the thermal bath of χ and ϕ has the same temperature as the SM thermal bath. The contact between those two sectors is provided by the Higgs portal $\lambda_4\varphi^2(H^\dagger H)$, providing interactions like $\phi\phi \leftrightarrow hh, \phi \leftrightarrow$

$hh, \phi\phi \leftrightarrow h$. If those interactions freeze out before χ decouples from ϕ, in principle the dark and visible sectors may acquire different temperatures due to a change in the number of relativistic degrees of freedom in the visible sector. Unless both, λ_4 and α, are extremely tiny, this may change the relic abundance by factors of order one compared to the situation presented above, while maintaining the qualitative picture. Various possibilities to obtain the relic abundance for various cases of DM and mediator properties have been discussed recently in [47]. Note that as long as the scalar mixing angle α is not exactly zero, H_2 is not stable and decays via the Higgs h into SM particles.

Hence, in this situation the Higgs portal acts indirectly, providing the link between the dark and visible thermal baths in the early universe. We call this "indirect Higgs portal". This situation is similar to secluded DM models [48], where DM annihilations into light mediator particles have been discussed, see also [49, 50]. A particular version of the indirect Higgs portal has been obtained in the model from [51]. That model respects a global $U(1)$ symmetry with a complex mediator ϕ, and the relic density may be set by the annihilation of DM into the massless Goldstone boson from the spontaneous breaking of the $U(1)$.

Let us mention that the inclusion of Sommerfeld enhancement in the computation of the DM relic density does not change qualitatively the general picture presented here. With respect to indirect detection searches, notice that the Sommerfeld correction is a velocity dependent effect that becomes larger when smaller velocities are involved. The Sommerfeld enhancement that affect dark matter annihilations in the galactic halo ($v \sim 10^{-6}$) is larger than $\bar{S}$ by several orders of magnitude. The annihilation cross sections involved in the scalar case are however always p-wave suppressed and we have checked that they for the model under study, they stay unconstrained by indirect detection searches.

4 Conclusions

Motivated by recent hints from LHC experiments for a SM-like Higgs particle around 125 GeV we have revisited here the possibility that the operator $(H^\dagger H)$ acts as a portal between the SM and the dark sector. We adopt the assumption that DM is a fermion, which necessarily requires additional degrees of freedom to couple it to the Higgs portal. We consider configurations where those additional particles are heavy and an EFT description is possible, as well as situations with light mediators. In the latter case we adopt a simple renormalizable toy model where a real scalar ϕ plays the role of the mediator particle. Assuming further that the DM relic abundance is obtained by thermal freeze-out in the early universe, the most simple realization of the fermionic Higgs portal DM is under pressure from constraints on the DM–nucleon scattering cross section from XENON100.

We have identified three simple ways to make thermal fermionic DM consistent with a SM-like Higgs at 125 GeV and XENON100 bounds:

- *Pseudo-scalar Higgs portal.* If DM couples to the Higgs portal via $\bar{\chi}\gamma_5\chi$ the direct detection cross section is suppressed by the DM velocity $\nu^2 \sim 10^{-6}$, whereas the annihilation cross section responsible for the relic abundance is unsuppressed.
- *Resonant Higgs portal.* If the DM mass m_χ is close to half of the Higgs mass m_h or the mediator mass m_ϕ, then the annihilation cross section is enhanced by an s-channel resonance, allowing for small couplings and a suppressed direct detection cross section.
- *Indirect Higgs portal.* If the mediator ϕ is lighter than the DM χ, the relic density can be obtained by $\chi\chi \leftrightarrow \phi\phi$ annihilations, where the t- and u-channel diagrams are independent of the Higgs portal strength. The Higgs portal only acts indirectly to provide thermal contact between the dark and the visible sector thermal baths.

In all cases it is possible to have a SM-like Higgs, with an LHC signal strength modifier $r_1 > 0.9$ (where $r_1 = 1$ corresponds to the SM Higgs). This framework is sometimes called "LHC nightmare scenario", with no new-physics signal at LHC apart from a SM-like Higgs. Also, by construction, the models discussed here can have unobservably small signals in direct detection experiments. However, in general a signal can be expected for indirect detection. For the pseudo-scalar and the indirect Higgs portals we predict a conventional indirect detection signal (dominated by annihilations into $\bar{b}b$ or gauge bosons), with an annihilation cross section determined by the thermal freeze-out of $\sigma\nu \simeq 3 \times 10^{-26}\,\mathrm{cm}^3\mathrm{s}^{-1}$. In the case of resonant Higgs portal there might be also an enhancement of the annihilation cross section today compared to the one in the early universe [52, 53] if the resonance is combined with a pseudo-scalar coupling. However, the enhancement effect may be not enough to overcome the velocity suppressed annihilation rate for pure scalar couplings.

In conclusion, fermionic Higgs portal DM remains a viable option if a SM-like Higgs should be established at the currently hinted mass of around 125 GeV. We have outlined simple mechanisms to obtain a classic "WIMP" DM candidate, whose relic abundance is set by thermal freeze-out, with no DM related signal at the LHC and highly suppressed rates in direct detection experiments, but still potentially observable in indirect detection.

Acknowledgement. We thank Joachim Kopp and Yasutaka Takanishi for useful discussions. L.L.H and T.S. acknowledge partial support from the European Union FP7 ITN INVISIBLES (Marie Curie Actions, PITN- GA-2011- 289442).

References

[1] B. Patt and F. Wilczek, *Higgs-field portal into hidden sectors*, (2006), hep-ph/0605188.

[2] Y. G. Kim and K. Y. Lee, *The minimal model of fermionic dark matter*, Phys. Rev. **D75**, 115012 (2007), hep-ph/0611069.

[3] J. March-Russell, S. M. West, D. Cumberbatch, and D. Hooper, *Heavy Dark Matter Through the Higgs Portal*, JHEP **07**, 058 (2008), 0801.3440.

[4] Y. G. Kim, K. Y. Lee, and S. Shin, *Singlet fermionic dark matter*, JHEP **0805**, 100 (2008), 0803.2932.

[5] M. Ahlers, J. Jaeckel, J. Redondo, and A. Ringwald, *Probing Hidden Sector Photons through the Higgs Window*, Phys. Rev. **D78**, 075005 (2008), 0807.4143.

[6] J. L. Feng, H. Tu, and H.-B. Yu, *Thermal Relics in Hidden Sectors*, JCAP **0810**, 043 (2008), 0808.2318.

[7] S. Andreas, T. Hambye, and M. H. G. Tytgat, *WIMP dark matter, Higgs exchange and DAMA*, JCAP **0810**, 034 (2008), 0808.0255.

[8] V. Barger, P. Langacker, M. McCaskey, M. Ramsey-Musolf, and G. Shaughnessy, *Complex Singlet Extension of the Standard Model*, Phys. Rev. **D79**, 015018 (2009), 0811.0393.

[9] M. Kadastik, K. Kannike, A. Racioppi, and M. Raidal, *EWSB from the soft portal into Dark Matter and prediction for direct detection*, Phys. Rev. Lett. **104**, 201301 (2010), 0912.2729.

[10] S. Kanemura, S. Matsumoto, T. Nabeshima, and N. Okada, *Can WIMP Dark Matter overcome the Nightmare Scenario?*, Phys.Rev. **D82**, 055026 (2010), 1005.5651.

[11] F. Piazza and M. Pospelov, *Sub-eV scalar dark matter through the super-renormalizable Higgs portal*, Phys. Rev. **D82**, 043533 (2010), 1003.2313.

[12] C. Arina, F.-X. Josse-Michaux, and N. Sahu, *A Tight Connection Between Direct and Indirect Detection of Dark Matter through Higgs Portal Couplings to a Hidden Sector*, Phys. Rev. **D82**, 015005 (2010), 1004.3953.

[13] I. Low, P. Schwaller, G. Shaughnessy, and C. E. Wagner, *The dark side of the Higgs boson*, Phys.Rev. **D85**, 015009 (2012), 1110.4405.

[14] A. Djouadi, O. Lebedev, Y. Mambrini, and J. Quevillon, *Implications of LHC searches for Higgs–portal dark matter*, (2011), 1112.3299.

[15] C. Englert, T. Plehn, D. Zerwas, and P. M. Zerwas, *Exploring the Higgs portal*, Phys.Lett. **B703**, 298 (2011), 1106.3097.

[16] J. F. Kamenik and C. Smith, *Could a light Higgs boson illuminate the dark sector?*, (2012), 1201.4814.

[17] M. Gonderinger, H. Lim, and M. J. Ramsey-Musolf, *Complex Scalar Singlet Dark Matter: Vacuum Stability and Phenomenology*, (2012), 1202.1316.

[18] O. Lebedev, *On Stability of the Electroweak Vacuum and the Higgs Portal*, (2012), 1203.0156.

[19] XENON100 Collaboration, E. Aprile *et al.*, *Dark Matter Results from 100 Live Days of XENON100 Data*, Phys.Rev.Lett. **107**, 131302 (2011), 1104.2549.

[20] CDMS Collaboration, EDELWEISS Collaboration, Z. Ahmed *et al.*, *Combined Limits on WIMPs from the CDMS and EDELWEISS Experiments*, Phys.Rev. **D84**, 011102 (2011), 1105.3377.

[21] ATLAS Collaboration, *Combined search for the Standard Model Higgs boson using up to 4.9 fb-1 of pp collision data at sqrt(s) = 7 TeV with the ATLAS detector at the LHC*, (2012), 1202.1408.

[22] CMS, S. Chatrchyan *et al.*, *Combined results of searches for the standard model Higgs boson in pp collisions at sqrt(s) = 7 TeV*, (2012), 1202.1488.

[23] J. R. Espinosa, C. Grojean, M. Muhlleitner, and M. Trott, *Fingerprinting Higgs Suspects at the LHC*, (2012), 1202.3697.

[24] A. Azatov, R. Contino, and J. Galloway, *Model-Independent Bounds on a Light Higgs*, (2012), 1202.3415.

[25] D. Carmi, A. Falkowski, E. Kuflik, and T. Volansky, *Interpreting LHC Higgs Results from Natural New Physics Perspective*, (2012), 1202.3144.

[26] Talks at Rencontres de Moriond EW, La Thuile, Italy, 3–10 March 2012, `http://indico.in2p3.fr/conferenceDisplay.py?confId=6001`

[27] M. Pospelov and A. Ritz, *Higgs decays to dark matter: beyond the minimal model*, Phys.Rev. **D84**, 113001 (2011), 1109.4872.

[28] S. Baek, P. Ko, and W.-I. Park, *Search for the Higgs portal to a singlet fermionic dark matter at the LHC*, JHEP **1202**, 047 (2012), 1112.1847.

[29] G. Belanger, F. Boudjema, A. Pukhov, and A. Semenov, *Dark matter direct detection rate in a generic model with micrOMEGAs2.1*, Comput. Phys. Commun. **180**, 747 (2009), 0803.2360.

[30] G. Belanger *et al.*, *Indirect search for dark matter with micrOMEGAs2.4*, Comput. Phys. Commun. **182**, 842 (2011), 1004.1092.

[31] Fermi-LAT collaboration, M. Ackermann *et al.*, *Constraining Dark Matter Models from a Combined Analysis of Milky Way Satellites with the Fermi Large Area Telescope*, Phys.Rev.Lett. **107**, 241302 (2011), 1108.3546.

[32] R. Kappl and M. W. Winkler, *Dark Matter after BESS-Polar II*, (2011), 1110.4376.

[33] M. Beltran, D. Hooper, E. W. Kolb, Z. A. Krusberg, and T. M. Tait, *Maverick dark matter at colliders*, JHEP **1009**, 037 (2010), 1002.4137.

[34] Y. Bai, P. J. Fox, and R. Harnik, *The Tevatron at the Frontier of Dark Matter Direct Detection*, JHEP **1012**, 048 (2010), 1005.3797.

[35] P. J. Fox, R. Harnik, J. Kopp, and Y. Tsai, *Missing Energy Signatures of Dark Matter at the LHC*, Phys.Rev. **D85**, 056011 (2012), 1109.4398.

[36] CMS Collaboration, S. Chatrchyan *et al.*, *Search for dark matter and large extra dimensions in monojet events in pp collisions at sqrt(s)= 7 TeV*, (2012), 1206.5663.

[37] C. Bird, R. V. Kowalewski, and M. Pospelov, *Dark matter pair-production in $b \to s$ transitions*, Mod.Phys.Lett. **A21**, 457 (2006), hep-ph/0601090.

[38] F. D'Eramo, *Dark matter and Higgs boson physics*, Phys.Rev. **D76**, 083522 (2007), 0705.4493.

[39] C. Englert, T. Plehn, M. Rauch, D. Zerwas, and P. M. Zerwas, *LHC: Standard Higgs and Hidden Higgs*, Phys. Lett. **B707**, 512 (2012), 1112.3007.

[40] A. Sommerfeld, Annalen der Physik **403**, 257 (1931).

[41] J. Hisano, S. Matsumoto, and M. M. Nojiri, *Explosive dark matter annihilation*, Phys.Rev.Lett. **92**, 031303 (2004), hep-ph/0307216.

[42] N. Arkani-Hamed, D. P. Finkbeiner, T. R. Slatyer, and N. Weiner, *A Theory of Dark Matter*, Phys.Rev. **D79**, 015014 (2009), 0810.0713.

[43] J. D. March-Russell and S. M. West, *WIMPonium and Boost Factors for Indirect Dark Matter Detection*, Phys.Lett. **B676**, 133 (2009), 0812.0559.

[44] C. Arina, F.-X. Josse-Michaux, and N. Sahu, *Constraining Sommerfeld Enhanced Annihilation Cross-sections of Dark Matter via Direct Searches*, Phys.Lett. **B691**, 219 (2010), 1004.0645.

[45] J. L. Feng, M. Kaplinghat, and H.-B. Yu, *Sommerfeld Enhancements for Thermal Relic Dark Matter*, Phys.Rev. **D82**, 083525 (2010), 1005.4678.

[46] K. L. McDonald, *Sommerfeld Enhancement from Multiple Mediators*, (2012), 1203.6341.

[47] X. Chu, T. Hambye, and M. H. Tytgat, *The Four Basic Ways of Creating Dark Matter Through a Portal*, (2011), 1112.0493.

[48] M. Pospelov, A. Ritz, and M. B. Voloshin, *Secluded WIMP Dark Matter*, Phys.Lett. **B662**, 53 (2008), 0711.4866.

[49] D. P. Finkbeiner and N. Weiner, *Exciting Dark Matter and the INTEGRAL/SPI 511 keV signal*, Phys.Rev. **D76**, 083519 (2007), astro-ph/0702587.

[50] Y. G. Kim and S. Shin, *Singlet Fermionic Dark Matter explains DAMA signal*, JHEP **0905**, 036 (2009), 0901.2609.

[51] M. Lindner, D. Schmidt, and T. Schwetz, *Dark Matter and Neutrino Masses from Global $U(1)_{B-L}$ Symmetry Breaking*, Phys.Lett. **B705**, 324 (2011), 1105.4626.

[52] M. Ibe, H. Murayama, and T. Yanagida, *Breit-Wigner Enhancement of Dark Matter Annihilation*, Phys.Rev. **D79**, 095009 (2009), 0812.0072.

[53] D. Feldman, Z. Liu, and P. Nath, *PAMELA Positron Excess as a Signal from the Hidden Sector*, Phys.Rev. **D79**, 063509 (2009), 0810.5762.